Journal of Materials Chemistry A

Accepted Manuscript

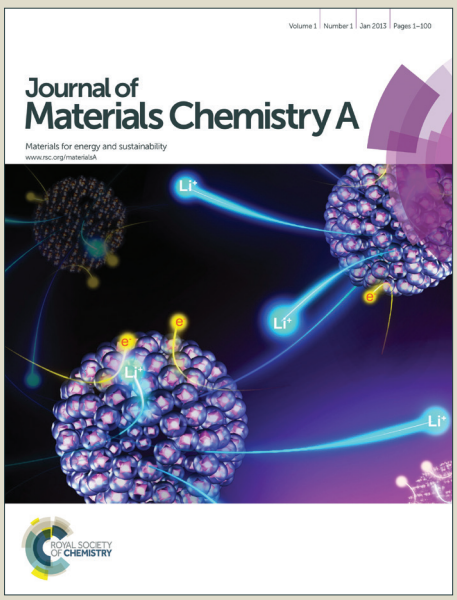

ROYAL SOCIETY OF CHEMISTRY

www.rsc.org/materialsA

Cite this: DOI: 10.1039/c0xx00000x

www.rsc.org/xxxxxx

ARTICLE TYPE

Rational Construction of Microporous Imide-Bridged Covalent–Organic Polytriazines for High-enthalpy Small Gas Absorption†

Shaofei Wu,[¥a] Shuai Gu,[¥a] Aiqing Zhang,[b] Guipeng Yu,*[a] Zhonggang Wang,*[c] Jigao Jian,[c] Chunyue Pan*[a]

Received (in XXX, XXX) Xth XXXXXXXXX 20XX, Accepted Xth XXXXXXXXX 20XX
DOI: 10.1039/b000000x

A series of microporous imide functionalized 1,3,5-triazine frameworks (named TPIs@IC) were designed by a easy-construction technology other than the known imidazation method for the construction of porous triazine-based polyimide networks (TPIs) with same chemical compositions. In contrast to TPIs, TPIs@IC exhibit much higher Brunauer-Emmett-Teller (BET) surface areas (up to 1053 m^2 g^{-1}) and carbon dioxide uptake (up to 3.2 mmol g^{-1}/14.2 wt% at 273K/1bar). The presence of abundant ultramicropores at 5.4~6.8 Å, mainly ascribed to a high-level cyano cross-linking, allows high heat absorption and high selective capture of CO_2. The Q_{st} (CO_2 esoteric enthalpies) from their CO_2 adsorptions isotherms at 273 and 298 K are calculated to be in the range 46.1-49.3 kJ mol^{-1} at low CO_2 loading, and ideal CO_2/N_2 separation factors are up to 151, exceeding those of most reported porous organic polymers to date. High storage capacities of TPIs@IC for other small gases like CH_4 (5.01 wt% at 298 K/22 bar) and H_2 (1.47 wt% at 77K/1bar) were also observed, making them promising adsorbents for gas adsorption and separation.

1. Introduction

A variety of solid sorbents including porous coordination polymers,[1] metal-organic frameworks (MOFs)[2] and porous organic polymers (POPs)[3] have been intensively investigated as potential materials for small gases (carbon dioxide, hydrogen and methane) capture for clean energy applications. The former two frameworks featuring huge surface areas and low cost exhibit attractive gas uptake capacity, but nevertheless always suffer from poor physical and chemical stability.[4] The main drawback of such sorbents is their low tolerance to water vapor that is usually present in the gas stream, which undoubtedly damages their practical popularity. POPs linked by strong covalent bonds instead of the coordination bonds exceed such limits and have been demonstrated as competent and promising candidates for small gas capture and storage relevant to clean energy.

POPs constructed solely from light elements like carbon and hydrogen often possess weak adsorption affinity towards guest molecules and hence low small gas uptake capacity. One intensively employed strategy to improve the small gases uptake is the pore surface engineering by introducing heteroatom functionalities to enhance the binding affinity between host and guest molecule.[5] 1,3,5-triazine and imide groups with high nitrogen content are deemed as ideal building blocks to develop high performance POPs.[6] Such porous polymeric materials, which can be separately synthesized via the cyclization polymerization of aromatic nitriles[7] or the condensation of amine and aromatic anhydrides,[8] are attractive for energy storage applications because of their high mechanical strength, as well as superior chemical and thermal stability compared to other porous organic macromolecules. Recently, Han et al reported a maximum CO_2-adsorption capacity of 5.53 mmol g^{-1} at 273 K and 1 bar for a perfluorinated covalent triazine-based framework.[7b] More importantly, its uptake of CO_2 reaches 1.76 mmol g^{-1} at 273 K and 0.1 bar with an initial Q_{st} value (35.0 kJ mol^{-1}). Our group recently applied the concept of polar electronic-rich groups such as triphenylamine, carbazole, dibenzofuran, and dibenzothiophene to covalent triazine-based frameworks and observed significantly improved adsorption performance for small gases (eg. CO_2 and H_2).[6b,9] On the other hand, remarkable progress has been achieved for the design and pore surface engineering of microporous aromatic polyimides.[10] We disclosed the preparation of microporous polyimide networks with BET surface areas up to 1407 m^2 g^{-1} derived from a rigid tetrahedral monomer tetra(4-aminophenyl)methane through imidazation technology in 2010.[10a] Such hypercrosslinked networks can absorb 3.30 wt% of H_2 at 77 K/35 bar. The highest reported surface area for a porous polyimide is 2213 m^2 g^{-1} derived from tetrahedrally organized perylene, which also showed 31 wt % of CO_2 at 195 K and 1 bar.[11] Impressively, Liebl and coworkers synthesized series of porous triazine-based polyimide networks (TPIs) combined with the attracting properties of two heterocyclic polymers.[12] TPIs show moderate BET surface areas ranging from 40 to 809 m^2 g^{-1} as well as broad pore size distribution and among of them the highest CO_2 uptakes are recorded to 2.45 mmol g^{-1} (10.8 wt%) at 273 K and 1 bar. Nevertheless, the inconvenience is that TPIs were obtained with a time-consuming and multi-step synthesis starting from high-

priced halo-substituted nitriles using noble metals as catalysts at a remarkably low overall yield (<35%). Additionally, the low porosity of TPIs together with their relatively low absorption capacities, which is strongly enslaved to the solubility of the respective dianhydride building block in toxic solvent mediums (like *m*-cresol), leaves a significant improvement of the carbon dioxide uptakes to be desired. Moreover, their hydrogen and methane storage performance still remain unexplored.

As part of an ongoing project dealing with porous polymers with tailor-made structures and properties, herein, we present a simple two-step synthetic strategy to alternatively build imide-based porous 1,3,5-triazine frameworks (TPIs@IC, namely TPIs synthesized under ionothermal condition) which have the same chemical composition as the disclosed TPIs at enhanced overall yields. Comparing with TPIs, considerably improved BET surface areas and carbon dioxide uptakes were demonstrated by TPIs@IC. TPIs@IC with abundant ultramicroporisity exhibit high carbon dioxide absorption heats (up to 49.3 kJ mol^{-1}), which are among the best reported results for porous organic polymers. Additionally, hydrogen and methane adsorption measurements for TPIs@IC show excellent uptake capacities despite their moderate BET surface areas.

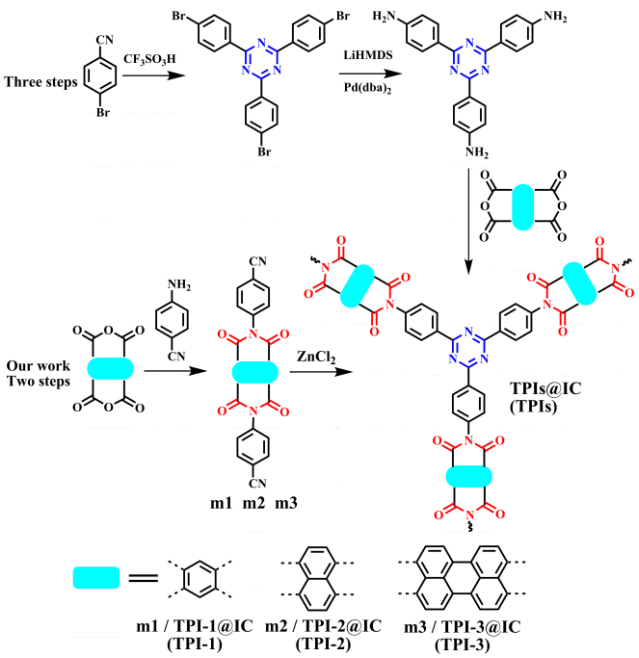

Fig. 1 Synthesis routes for TPIs@IC (TPIs).

2. Experimental

General procedure for the preparation of TPIs@IC

The polymeric networks were synthesized by heating a mixture of 1 g monomer and $ZnCl_2$ (molar ratio, $ZnCl_2$: monomer=10:1) in a quartz tube (3×10 cm). The tube was evacuated to a high vacuum, and then sealed rapidly. TPI-1@IC was synthesized by a selected temperature program (Table S1, ESI†) (200 °C/5 h, 300 °C/5 h, 400 °C/20 h), while TPI-2@IC was obtained by a temperature program (200 °C/5 h, 300 °C/5 h, 400 °C/10 h, 450 °C/10 h, 500 °C/20 h), and the temperature program for TPI-3@IC (200 °C/5 h, 300 °C/5 h, 400 °C/10 h, 450 °C/10 h, 500 °C/10 h, 600 °C/20 h) was utilized afterwards. The quartz tube was then cooled to room temperature and opened. The reaction mixture was subsequently ground, and then washed thoroughly with water to remove most of $ZnCl_2$. Further stirring in diluted HCl for 15 h was carried out to remove the residual salt. After this purification step, the resulting black powder was filtered, and washed successively with water and methyl alcohol, following by Soxhlet extraction using acetone, methyl alcohol and hexane as eluting solvents sequentially, and dried in vacuum at 150 ℃. Typical isolated yields >90%.

3. Results and discussion

The synthesis routes for microporous imide-functionalized 1,3,5-triazine frameworks (TPIs@IC) and the reported porous triazine-based polyimide networks (TPIs) are illustrated in Figure 1. All TPIs@IC were readily prepared by a two-step reaction starting from 4-aminobenzonitrile and respective aromatic dianhydrides with overall yields ranging from 56% to 82%, whereas those of TPIs were apparently much lower (31-35%). The rigid nitrile-functioned precursors (m_1, m_2, m_3) were synthesized by one-step solution condensations of 4-aminobenzonitrile (A) with corresponding rigid aromatic anhydrides (Fig. 1). The progress of the reactions was confirmed by ^{1}H NMR and MALDI-TOF/MS measurements. On the contrary, for TPIs the time-consuming synthesis of 4,4',4''-(1,3,5-triamine-2,4,6-triyl)trianiline block was accomplished in the catalysis of corrosive super acid (CF_3SO_3H) and volatile organometalliic reagents (LiHMDS and $Pd(dba)_2$), indicating their harsh reaction conditions and costly synthetic procedures, which undoubtedly limits their possibility for scale up. Additionally, TPIs were constructed via the known imidazation technology of the aromatic dianhydride and aromatic triamines in low boiling point organic solvent mediums (i.e. *m*-cresol). Although such polymerization is easier to handle, no high level of cross-linking was achieved for TPIs. This could be easily explained, considering the restricted reaction temperatures by organic mediums and the crystallization or precipitation of the intermediates prior to the formation of the highly crosslinked networks. We surmised that such higher surface area, porous organic materials could be achieved by increasing the degree of cross-linking of the function groups. Indeed, previous reports on microporous hyper-crosslinked organic polymers have suggested that higher level of cyano cross-linking and hence much higher network rigidity can lead to higher surface areas for the resulting materials.[15,22]

Although our dinitrile compounds display poor solubility in common solvent such as hexane, chloroform, acetone, DMSO and DMF, they are highly miscible in molten $ZnCl_2$ and strong acids. Unfortunately, our efforts to accomplish their polymerization using trifluoromethanesulfonic acid as catalyst under room temperature failed to obtain objective highly crosslinked networks. This fact may be reasonable considering that the magic acid has caused breakage within C-N and C-O linkages of the heterocyclic-containing nitriles. We describe herein a simple approach for producing TPIs@IC which has been proved to be very valuable for building highly porous organic polytriazines from thermal/chemical unstable blocks.[9] The hyper-crosslinked polytriazines were synthesized from aromatic nitriles

in sealed quartz ampoules via multiply-step heating programs (Table S1, ESI†). Comparing with the *m*-cresol applied for TPIs, molten $ZnCl_2$ is a much better solvent for monomers and triazine-based oligomers owing to strong Lewis acid-base interactions. Furthermore, molten $ZnCl_2$ has been shown to be an excellent solvent for the syntheses of polytriazines, since allowing extremely high temperatures (eg., 600 ^oC, etc) which is required to maintain high-degree cross-linking through the trimerization of cyano groups. The heating programs for the polymerization of nitrile-functioned precursors were optimized to obtain hyper-crosslinked networks with good porosity (Table S1, ESI†). In cases of naphthalene-centred nitrile and perylene-centred nitrile, the polymerizations under the conditions similar to those for TPI-1@IC, only gave soluble products without permanent porosity. When a higher reaction temperature is used (500 or 600 ℃, Table S1, ESI†, entries 4, 5 and 6), it was possible to isolate insoluble networks from the reaction system.

Three TPIs@IC were coincidently obtained as black monolithic materials in almost quantitative yields. They are insoluble in water and common organic solvents such as hexane, methanol, acetone, chloroform, *N*,*N*-dimethylacetamide (DMAc), *N*-methylpyrroli-done (NMP), and tetrahydrofuran (THF) along with diluted HCl solution (10 wt%), implying their good chemical stability. The imide functionality of these networks were further analyzed by the spectral measurements. For instance, in the FT-IR spectrum of TPI-3@IC (Fig. 1S) the structure of imide functionality is confirmed by the characteristic bands at 1658 cm^{-1} corresponding to the vibrations of the C=O group in five-membered polyimide rings, which is in good accordance with the solid-state CP/MAS NMR measurement. The broad band at about 1310-1380 cm^{-1} correlates to overlap of the C-N-C stretching vibration of the imide ring and the in-plane stretching vibration of the triazine ring. For all polymers, the disappearance of the absorption around 2235 cm^{-1} in FT-IR spectra ascribing to the characteristic carbonitrile stretching suggests almost completely conversion of cyano groups under the investigated conditions, while the appearance of strong absorption bands at 1360 and 1508 cm^{-1} is indicative of a successful trimerization reaction. The FTIR spectra and BET surface areas of the samples after refluxing in HCl solution (10 wt%) for 48 h are all kept comparing with the original networks, further confirmed the retentivity of the structure. According to other relevant literatures,[7d,7e,9] some materials of this type failed to obtain a meaningful solid-state CP/MAS NMR spectrum. For example, the spectrum of TPI-2@IC (Fig. 2S) only gives characteristic peaks of aromatic carbons (at 125 ppm) and carbonyl carbons in polyimide rings (at 162 ppm), while no fine-structure resolution was found. Nitrogen and oxygen elimination during the polymerization reaction were observed from elemental analysis (Table S2, ESI†). These deviations may be reasonable considering the incomplete combustion and trapped adsorbates including gases and water vapour.[7] Inductively Coupled Plasma (ICP) analysis shows 6.7 wt%, 6.1 wt% and 5.9 wt% zinc contents for TPI-1@IC, TPI-2@IC and TPI-3@IC, respectively (Table S2, ESI†), which are reasonable and slightly higher than those of reported NPTNs (4.7~5.9 wt%).[9] Morphologies monitored by scanning electron microscopy (SEM, Fig. S3-S5, ESI†) demonstrate that TPI-1@IC displays a floppy surface and TPI-2@IC exhibits a compact surface, while a strip sponge-like morphology was observed for TPI-3@IC. The microstructure is studied by high-resolution transmission electron microscopy (HR-TEM) and X-ray powder diffraction (PXRD). Typically, alternately dark and bright area can be clearly observed for TPIs@IC, implying porous structure (Fig. S6-S8, ESI†). The PXRD spectra of all networks give an amorphous feature (Fig. S9-S11, ESI†). Thermo-gravimetric measurements (Fig. S12, ESI†) show that all three networks deliver excellent thermodynamic stability, with 5% weight loss exceeding 450 ^oC. To note out, TPIs@IC still show char yields of over 75% when heated to 800 ^oC under a nitrogen atmosphere.

To characterize the porosity of TPIs@IC, cryogenic nitrogen adsorption isotherms were collected at 77 K (Fig. 2). TPI-1@IC performs a Type I isotherm in the range of P/P_0= 0.05-0.15, and then possess a very flat adsorption plateau, suggesting the microporous nature. Notably, TPI-1@IC displays some Type II character with a rise in the nitrogen sorption at high relative pressures (P/P_0>0.9). As a sharp contrast, TPI-2@IC and TPI-3@IC exhibit typical Type II gas sorption isotherms as well as an obvious hysteresis phenomenon, which might be attributed to the existence of meso-pore structure and interparticulate voids of the samples. The isotherms for all TPIs@IC exhibit a sharp N_2 adsorption at low relative pressures (P/P_0<0.01), implying the existence of abundant micropores and ultramicropores. Applying the Brunauer-Emmett-Teller (BET) model to these isotherms gives apparent surface areas of 1053 $m^2\ g^{-1}$, 814 $m^2\ g^{-1}$ and 963 $m^2\ g^{-1}$ for TPI-1@IC, TPI-2@IC and TPI-3@IC, respectively (Table 1). The slightly decreased surface area for TPI-2@IC and TPI-3@IC relative to TPI-1@IC could be due to the following two reasons: the volume of naphthalene in TPI-2@IC and perylene in TPI-3@IC is obviously larger than the benzene strut; second, the pi-stacking of the naphthalene and perylene groups is also unfavorable for the pore formation because of the strong *p*-electron-delocalization effect. The BET surface areas of TPIs@IC are sufficiently higher than the values reported for TPI-1 (809 $m^2\ g^{-1}$), TPI-2 (796 $m^2\ g^{-1}$) and TPI-3 (40 $m^2\ g^{-1}$) of the same chemical composition. A plausible explanation for this is that the high degree of crosslinking and hence high network rigidity effectively prevent the tight packing or entanglement of chains, thus resulting in high BET surface areas as discussed above.

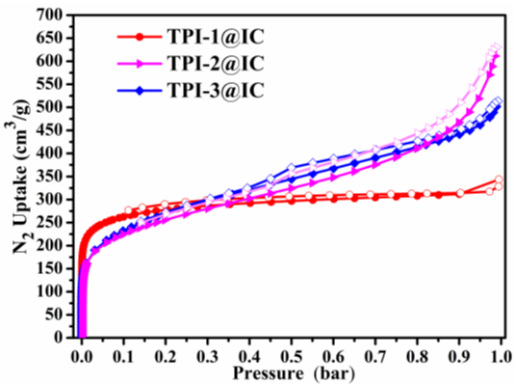

Fig.2 N_2 adsorption (solid symbols)/desorption (open symbols) isotherms at 77K

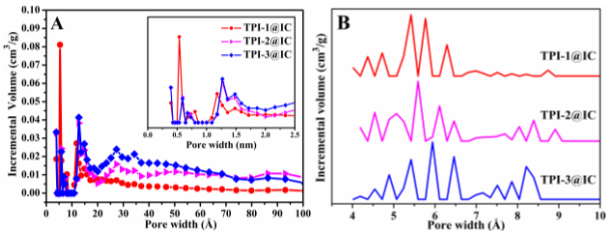

Fig.3 NLDFT pore size distribution of TPIs@IC from (A) N_2 adsorption (at 77 K) and (B) CO_2 adsorption (at 273 K).

Pore size distribution (PSD) of N_2 adsorption at 77 K (Fig. 3A) was estimated from the nonlocal density functional theory (NLDFT),[13] while pore volume was calculated from single point measurements (P/P_0=0.97) and found to be 0.53, 0.76, and 0.74 $cm^3\ g^{-1}$ for TPI-1@IC, TPI-2@IC and TPI-3@IC, respectively. TPIs@IC show higher pore volume than that of TPIs suggesting improved gas capacity, which was further confirmed by their carbon dioxide adsorption isotherms at 298 and 273 K (Fig. 3). It is interesting to observe that all TPIs@IC possess abundant micropores and supermicropores. TPI-1@IC exhibits a narrow pore-size distribution and abundant micropore and supermicropore with pore diameters centered at around 1.48 nm and 0.54 nm, respectively. Interestingly, TPI-2@IC and TPI-3@IC show similar PSD curves with dominant pore width located at 0.59 nm and 1.27 nm in addition to spot mesopores peaked at 2.7 nm. One possible application for the small pore size is that the subdividing of the cavity by the segments or rigid strut moieties because of the network interpenetration. The formation of an additional mesopore system for TPI-3@IC, which leads to a drastic increase of the surface area, may be due to another mode of self-organization of the system at higher temperatures.[14] In consideration of the advantages of the CO_2 sorption-based model for pore size distribution (PSD) below 1 nm,[7d] CO_2 micropore analysis data at 273 K was calculated with NLDFT approach and exhibits dominant pore width of TPIs@IC range from 0.4 nm to 0.7 nm (Fig. 3B), further demonstrating that ionothermal method facilitates the formation of ultra-micropores. Comparing with PSD profiles of TPI-2@IC and TPI-3@IC, the curve of TPI-1@IC without intense peaks at 0.7~1 nm displays more single-minded pore size distribution at supermicropore range (<0.7 nm), implying a strong CO_2 adsorption potential for TPI-1@IC.

Table 1. Pore parameters and CO_2 uptake of TPIs@IC and TPIs

Polymer	S_{BET}[a] m^2/g	S^b_{LAN} m^2/g	V_{Total}[c] cm^3/g	Pore Size[d] nm	CO_2 uptake[e] 273 K	298 K
TPI-1@IC	1053	1295	0.53	0.54, 1.48	3.22	2.11
TPI-2@IC	814	1059	0.76	0.58, 1.27, 2.7	2.06	1.43
TPI-3@IC	963	1316	0.74	0.58, 1.27, 2.7	2.17	1.44
TPI-1[f]	809	-	0.45	0.75-0.85	2.45	1.25
TPI-2[f]	796	-	0.40	0.75-0.85	2.45	1.23
TPI-3[f]	40	-			0.68	0.43

[a]Brunauer-Emmett-Teller surface area. [b]Langmuir surface area. [c]Pore volume determined from the N_2 isotherm at P/P_0=0.99. [d]Pore size derived from N_2 isotherm with the NLDFT approach. [e]In mmol/g at 1 bar. [f]Results from Ref 12.

As we estimated, TPI-1@IC and TPI-3@IC exhibit carbon dioxide adsorption of 3.22 and 2.17 mmol g^{-1} under 1 bar and at 273 K (Fig. 4), respectively, which are almost two times of TPI-1 (2.45 mmol g^{-1}) and TPI-3 (0.68 mmol g^{-1}) (Table 1). At elevated temperatures (eg. 298 K), the carbon dioxide uptake capacities of TPI-1@IC (2.11 mmol g^{-1}) and TPI-3@IC (1.44 mmol g^{-1}) are slightly decreased under 1 bar, and are also sufficiently higher than those reported for TPI-1 (1.25 mmol g^{-1}) and TPI-3 (0.43 mmol g^{-1}). This may indicate that narrow ultramicropores (<1 nm) make a superior contribution to CO_2 adsorption than wide micropores and mesopores of TPIs, considering their same pore surface nature and thermodynamic size of CO_2.[7] It is worth mentioning that the uptake capacity of TPI-1@IC at 1 bar and 273 K surpasses those of other heteroatom-containing materials, including 1,3,5-triazine based conjugated microporous polymers TCMPs (1.22-2.62 mmol g^{-1}),[15] azo-linked covalent organic polymers azo-COPs (1.93-2.55 mmol g^{-1}),[16] NOPs(1.31-2.80 mmol g^{-1}),[6a,6b] NPTNs(2.23-3.20 mmol g^{-1}),[9] and triptycene-based microporous poly(benzimidazole) networks TBIs (2.68-3.17 mmol g^{-1}).[17] We attribute this excellent carbon dioxide sorption capability of TPI-1@IC to the combination of appropriate pore volume and abundant narrow ultramicropores, which afford strong adsorption potential. In comparison with TPI-1@IC, TPI-3@IC possesses lower carbon dioxide uptake due to the existence of mesopores peaked at 2.7 nm, which might be too large to increase the number of double or multiple interactions between the adsorbed CO_2 and the pore walls.[18]

With the lowest BET surface area of TPIs@IC, TPI-2@IC displays the bottommost carbon dioxide loading (2.06 mmol g^{-1} at 273 K/1 bar). This could be attributed to the low degree of polymerization correlated to the limited solubility of m2 monomer. With higher temperature, such monomers show a better solubility in $ZnCl_2$ ionic melts owing to strong Lewis acid-base interaction, which also contributes to the dissolution of oligomers. At a temperature of 400 °C, for instance, the expected polymers were not obtained with the precursors m2 and m3 due to their poor solubility, while the temperature was adjusted to 500 °C, we gained TPI-2@IC with the lowest BET surface area of 814 $m^2\ g^{-1}$. Increasing the reaction temperature to 600 °C resulted in a successful construction of TPI-3@IC with a BET surface area of 963 $m^2\ g^{-1}$. This would be due to the high melting point of perylene-centred nitrile as well as good dissociation of the metal-organic complexes prior to consecutive reaction by high temperature cyclization.[14] Moreover, comparing to the preparation of TPIs in *m*-cresol at 190 °C,[12] the synthesis of TPIs@IC in ionic melt is more effective. Although heated to 190 °C (near the boiling temperature 202.3 °C), *m*-cresol remains a deficient solvent for the generation of highly crosslinked network.

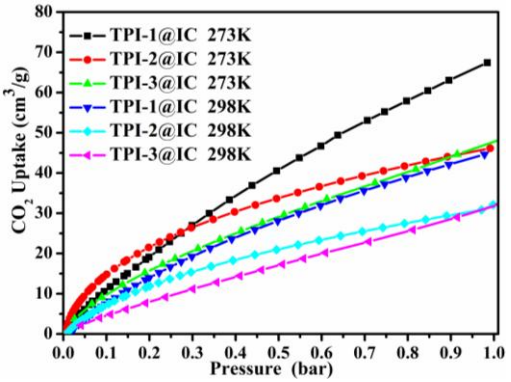

Fig. 4 CO_2 adsorption isotherms of TPIs@IC.

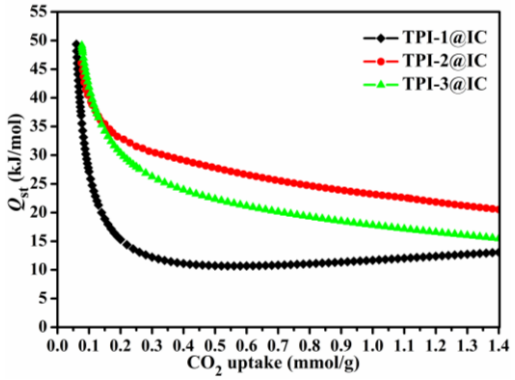

Fig. 5 Q_{st} from CO_2 adsorption at 273 and 298K.

TPI-3 with sufficient rigidity exhibits a carbon dioxide uptake of 0.68 mmol g^{-1} at 1 bar and 273 K (Table 1), apparently lower than our TPI-3@IC which has the same chemical composition. Therefore, the imidazation technology limits the number of suitable building blocks for this synthesis pathway. This demonstrates that our method for doping heteroatom into frameworks may be more impactful than that used for constructing high performance microporous organic polymers.

To determine the binding affinity of TPIs@IC for CO_2, we calculated the isosteric heats of adsorption for CO_2 from the data collected at 273 K and 298 K using the Clausius-Clapeyron equation (Fig. 5).[19] The isosteric heats determined at low loading were 49.3 kJ mol^{-1} for polymer TPI-1@IC, 46.1 kJ mol^{-1} for polymer TPI-2@IC and 49.1 kJ mol^{-1} for polymer TPI-3@IC, which were significantly improved compared to TPIs (29.2-34.4 kJ mol^{-1}),[12] HCPs (20.0-24.0 kJ mol^{-1}),[20] MCTFs (20.5-26.3 kJ mol^{-1}),[7a] BILPs (26.5-28.8 kJ mol^{-1}),[21] BLPs (20.2-28.3 kJ mol^{-1}),[22] CPOP-1 (27.0 kJ mol^{-1}),[5a] networks (23.3-28.2 kJ mol^{-1})[23] and STPIs (28-36 kJ mol^{-1})[8b] and SMPs (23.0-32.0 kJ mol^{-1}).[24] The exceptionally high Q_{st} values can be ascribed to the electron-rich imide rings and high charge density at nitrogen and oxygen sites that facilitates framework-gas interactions through hydrogen bonding and/or dipole-quadrupole interactions. With the CO_2 adsorption increasing from 0 mmol g^{-1} to 0.3 mmol g^{-1}, a rapid decrease was observed for these adsorption heat curves, indicating that the framework-gas interaction is more powerful than gas-gas interaction. Those profiles keep smooth at high adsorbed amount because of pure gas-gas interactions. Interestingly, the initial adsorption heats of TPIs@IC are approximately equal due to the similar ultramicropore and micropore size in addition to the similar chemical composition. TPI-2@IC and TPI-3@IC exhibit considerably higher isosteric heats than TPI-1@IC over a wide range of gas loadings, suggesting that the incorporation of strong *p*-electron-delocalization effect into the framework indeed enhances the host affinity towards CO_2.

To evaluate the adsorption selectivity of TPIs@IC for postcombustion flue gas, the prevalent ideal adsorbed solution theory (IAST) model was adopted to imitate the selectivity of CO_2 over N_2 at an equilibrium partial pressure of 0.85 bar (N_2) and 0.15 bar (CO_2) in the bulk phase (Fig. S13–S18, ESI†). The data in Table 2 show that ideal selectivities at 273 K/1 bar for

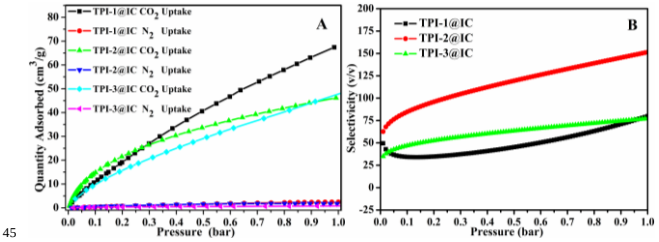

Fig. 6 A: Adsorption isotherms of CO_2 and N_2 gases at 273 K. B: IAST selectivities of CO_2 over N_2 for binary gas mixtures 15/85 molar composition in TPIs@IC at 273k.

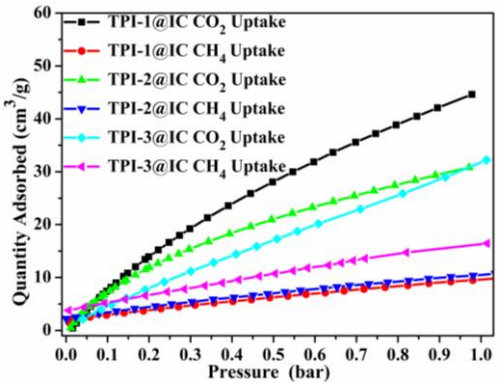

Fig. 7 Adsorption isotherms of CO_2 and CH_4 gases at 298 K

CO_2/N_2 gas mixture are 80, 151 and 77 for TPI-1@IC, TPI-2@IC and TPI-3@IC, respectively (Fig. 6B). The values are comparable to NOPs (53-81),[6b] pyrrole-HCP (117)[23] and FCTF-1-600 (152),[7b] superior to many other porous polymers like NPTNs (22-45),[9] PI-NDAT (25),[8c] PI-NO_2 (18-31)[8c] and networks (26-119).[23] For the sake of comparing the performance of our TPIs@IC and the known TPIs on selectively separation of small gases, we also calculated the CO_2 uptake and selectivity over N_2 involves the use of initial slope ratios estimated from Henry's law constants for single-component adsorption isotherms at 273 K (Fig. 6A). Based on this, we calculated the adsorption selectivity for CO_2 over N_2 in the pressure range below 0.15 bar (Fig. S19-S21, ESI†) and the results are presented in Table 2. TPI-1@IC, TPI-2@IC and TPI-3@IC show CO_2/N_2 selectivity ratios of 33, 70 and 55, respectively, which are higher than those of TPI-1 (31), TPI-2 (34) and TPI-3 (35). In comparison with the slightly large pore size of TPIs, the ample micropores and supermicropores of TPIs@IC, which match the dimension of CO_2 better for gas sorption, contribute a lot to the high CO_2/N_2 selectivity.

To further evaluate the potential use of TPIs@IC in gas separation applications, the selectivity of TPIs@IC toward CO_2 over CH_4 was investigated by collecting isotherms at 298 K (Fig. 7). At 298 K and 1 bar, TPI-1@IC, TPI-2@IC and TPI-3@IC exhibit CO_2 uptakes of 2.11, 1.43 and 1.44 mmol g^{-1}, respectively, whereas CH_4 adsorptions of TPI-1@IC (0.020 mmol g^{-1}), TPI-2@IC (0.021 mmol g^{-1}) and TPI-3@IC (0.034 mmol g^{-1}) are almost negligible. On the basis of initial slope calculations in the pressure range of 0 to 0.2 bar (Fig. S22-S24, ESI†), the estimated adsorption selectivity for CO_2 over CH_4 are 11, 8 and 2 (Table 2). The values of TPI-1@IC and TPI-2@IC exceed those reported for activated carbon and ZIFs. The high selectivity of CO_2 over N_2 and over CH_4 indicates that TPIs@IC are promising

Table 2. CO_2, H_2 and CH_4 sorption of TPIs@IC

Polymer	$S_{CO2/N2}$[a]	$S_{CO2/N2}$[b]	$S_{CO2/CH4}$[c]	Q_{st} kJ/mol	H_2 uptake[d] mmol/g	CH_4 uptake[e] 1 bar	22 bar
TPI-1@IC	80	32.2	11	49.3	6.15	0.020	2.04
TPI-2@IC	151	69.6	8	46.1	6.80	0.021	1.61
TPI-3@IC	77	55.1	2	49.1	7.35	0.034	3.13
TPI-1[f]	ND[g]	30.9	ND	34.4	ND	ND	ND
TPI-2[f]	ND	33.5	ND	31.4	ND	ND	ND
TPI-3[f]	ND	35.1	ND	ND	ND	ND	ND

[a]S_{CO2-N2} is calculated by the IAST model from 85% N_2 and 15% CO_2, at 1 bar/ 273 K. [b]S_{CO2-N2} is calculated from initial slope calculations at 273K. [c]$S_{CO2-CH4}$ is calculated from initial slope calculations at 298K. [d]at 77 K/1 bar. [e]in mmol g^{-1}. [f]Results from Ref 12. [g]No detection.

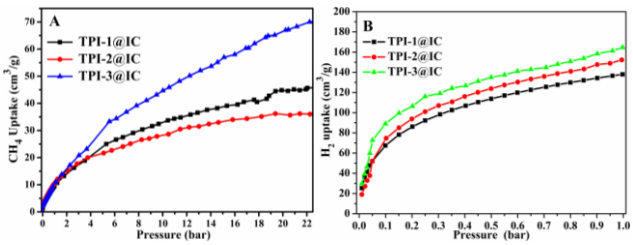

Fig. 8 Adsorption isotherms of CH_4 at 298K (A) and H_2 at 77K (B)

candidates for the separation and purification of CO_2 from various CO_2/CH_4 or CO_2/N_2 mixtures.

We have also considered TPIs@IC in hydrogen absorption and high pressure methane storage studies because both gases are attractive candidates for renewable and clean energy. The methane uptakes for TPIs@IC (1.61-3.13 mmol g^{-1}) at 298 K/22 bar (Fig. 8A) are comparable to COF-1 (2.5 mmol g^{-1}, 298 K/85 bar),[25] zeolites (1.94-4.56 mmol g^{-1}, 298 K/85 bar)[26] and mesoporous silicas (2.5 mmol g^{-1}, 298 K/85 bar).[26] Hydrogen storage capacity for TPIs@IC are 1.23 wt%, 1.36 wt% and 1.47 wt%, respectively, measured at 77 K and 1.0 bar (Fig. 8B). Similar to the CO_2 and CH_4 isotherms, the H_2 uptake has not reached saturation in the investigated pressure range, implying that high storage can be expected at higher pressures. The calculated hydrogen uptake ability is obviously higher than those reported for COF-11À (1.22 wt%),[27] EOFs (0.94-1.21 wt%),[28] polyanilines (0.38-0.85 wt%),[29] Porph-PIM (1.20 wt%),[30] PIM-1 (0.95 wt%),[30a,31] HCP-BDM (1.11 wt%)[32] and HCP-BA (0.97 wt%).[32] The high adsorption capacity of TPIs@IC can refer to their narrow ultra-micropores as well as polar surface due to the presence of triazine and imide rings.

4. Conclusions

We have demonstrated a facile method for the rapid and cost-effective synthesis of highly microporous imide functionalized 1,3,5-triazine frameworks (TPIs@IC) other than the deficient imidazation method. The obtained networks, which have the same chemical compositions as the known TPIs, exhibit higher BET surface areas (up to 1053 m^2 g^{-1}) and better carbon dioxide uptake ability (up to 3.2 mmol g^{-1}/14.2 wt%). The presence of abundant ultramicropores affords TPIs@IC with remarkably high absorption enthalpies (up to 49.3 kJ mol^{-1}) as well as high selectivities: CO_2/N_2 (151 at 273 K) based on IAST calculations and CO_2/CH_4 (11 at 298 K) derived from the ratios of initial slopes of isotherms, making them very attractive in CO_2 adsorption and separation studies. TPIs@IC can also store up to 7.35 mmol g^{-1} H_2 at 77 K/1 bar and 3.13 mmol g^{-1} CH_4 at 298 K/22 bar, comparable with many other porous organic polymers. The synthetic availability, structural precision and highly microporous nature open a new opportunity for the large-scale industrial preparation of high performance carbonaceous absorbents and their application in small gas absorption and separation.

Acknowledge

We acknowledge the financially support from the National Science Foundation of China (Nos. 21204103 and 21376272), China Postdoctoral Science Foundation (2012M521535), China Postdoctoral Science Foundation Specialized Funded project (2014T70787), State Key Laboratory of Fine Chemicals (KF1206), Key Laboratory of Catalysis and Materials Science of the State Ethnic Affairs Commission & Ministry of Eduction (CHCL12006), and State Key Laboratory of Advanced Technolgy for Materials and Processing (2015-KF-8).

Notes and references

[a]*College of Chemistry and Chemical Engineering , Central South University, Changsha 410083, China. E-mail:gilbertyu@csu.edu.cn; panchunyue@sina.com.*
[b]*Key Laboratory of Catalysis and Materials Science of the State Ethnic Affairs Commission & Ministry of Eduction, Hubei Province, South-Central University for Nationalities, Wuhan 430074, P. R. China*
[c]*Department of Polymer Science & Materials, State Key Laboratory of Fine Chemicals, Dalian University of Technology, Dalian 116012, China.*
¥These authors contribute to this work equally.
† Electronic Supplementary Information (ESI) available: [Synthesis and Characterization data and properties]. See DOI: 10.1039/b000000x/

1 (a) P. Li, Y.-B. He, J Guang, L.-H Weng, J. C.-G. Zhao, S. C. Xiang and B. L. Chen, *J. Am. Chem. Soc.*, 2014, **136**, 547–549. (b) M. Mastalerz and I. M. Oppel, *Angew. Chem., Int. Ed.*, 2012, **51**, 5252-5255.
2 (a) A. M. Fracaroli, H. Furukawa, M. Suzuki, M. Dodd, S. Okajima, F. Gandara, J. A. Reimer and O. M. Yaghi, *J. Am. Chem. Soc.*, 2014, **136**, 8863-8866. (b) F. Gandara, H. Furukawa, S. Lee and O. M. Yaghi, *J. Am. Chem. Soc.*, 2014, **136**, 5271-5274. (c) F. Jeremias, V. Lozan, S. K. Henninger and C. Janiak, *Dalton Trans.*, 2013, **42**, 15967-15973. (d) K. Schutte, H. Meyer, C. Gemel, J. Barthel, R. A. Fischer and C. Janiak, *Nanoscale*, 2014, **6**, 3116-3126.
3 (a) Y. Yuan, F.-X. Sun, L. Li, P. Cui and G.-S. Zhu, *Nat. Commun.*, 2014, **5**, 4260-4267. (b) X. Gao, X.-Q. Zou, H.-P. Ma, S. Meng and G.-S. Zhu, *Adv. Mater.*, 2014, **26**, 3644–364. (c) S.-Y. Ding and W. Wang, *Chem. Soc. Rev.*, 2013, **42**, 548-568. (d) X.-H. Liu, C.-Z. Guan, S.-Y. Ding, W. Wang, H.-J. Yan, D. Wang and L.-J. Wan, *J. Am. Chem. Soc.*, 2013, **135**, 10470-10474.
4 H.Furukawa, K. E. Cordova, M. O. Keeffe and O. M. Yaghi, *Science*, 2013, **341**, 1230444-1-1230444-12.
5 (a) Q. Chen, M. Luo, P. Hammersh øj, D. Zhou, Y. Han, B. W. Laursen, C.-G. Yan and B.-H. Han, *J. Am. Chem. Soc.*, 2012, **134**, 6084–6087. (b) Q. Chen, D.-P. Liu, M. Luo, L.-J. Feng, Y.-C. Zhao and B.-H. Han, *Small*, 2014, **10**, 308-315.
6 (a) S.-H. Xiong, X. Fu, L. Xiang, G.-P. Yu, J. G. Guan, Z.-G Wang, Y. Du, X. Xiong and C.-Y Pan, *Polym. Chem.*, 2014, **5**, 3424–3431. (b) Y. Liu, S.-F. Wu, G. Wang, G.-P. Yu, J. G. Guan, C.-Y Pan and Z.-G Wang, *J. Mater. Chem. A.*, 2014, **2**, 7795-7801. (c) L. Stegbauer, K. Schwinghammer and B. V. Lotsch, *Chem. Sci.*, 2014, **5**, 2789-2793. (d)G.-Y. Li and Z.-G Wang, *Macromolecules*, 2013, **46**, 3058-3066.
7 (a) X.-M. Liu, H. Li, Y.-W. Zhang, B. Xu, Sigen A, H. Xia and Y. Mu, *Polym. Chem.*, 2013, **4**, 2445–2448. (b) Y.-F. Zhao, K.-X. Yao, B.-Y. Teng, T. Zhang and Y. Han, *Energy Environ. Sci.*, 2013, **6**, 3684–3692. (c) Sevilla, M.; Valle-Vigón, P.; Fuertes, A. B. *Adv. Funct. Mater.* 2011, **21**, 2781−2787. (d) A. Bhunia, I. Boldog, A.

Moller and C. Janiak, *J. Mater. Chem. A.*, 2013, **1**, 14990-14999. (e) A. Bhunia, V. Vasylyeva and C. Janiak, *Chem. Commun.*, 2013, **49**, 3961-3963.

8 (a) C. J. Shen, Y.-J. Bao and Z.-G Wang, *Chem. Commun.*, 2013, **49**, 3321-3323. (b) C. Zhang, T.-L. Zhai, J.-J. Wang, Z. Wang, J.-M. Liu, B.-E. Tan, X.-L. Yang and H.-B. Xu, *Polymer*, 2014, **55**, 3642-3647. (c) C.-J. Shen and Z.-G. Wang, *J. Phys. Chem. C*, 2014, **118**, 17585-17593.

9 S.-F. Wu, Y. Liu, G.-P. Yu, J.-G. Guan, C.-Y. Pan, Y. Du, X. Xiong and Z.-G. Wang, *Macromolecules*, 2014, **47**, 2875-2882.

10 (a) Z.-G. Wang, B.-F. Zhang, H. Yu, L.-X. Sun, C.-L. Jiao and W.-S. Liu, *Chem. Commun.*, 2010, **46**, 7730-7732. (b) J. Weber, Q. Su, M. Antonietti and A. Thomas, *Macromol. Rapid Commun.*, 2007, **28**, 1871-1876. (c) B. S. Ghanem, N. B. McKeown, P. M. Budd, N. M. Al-Harbi, D. Fritsch, K. Heinrich, L. Starannikova, A. Tokarev and Y. Yampolskii, *Macromolecules*, 2009, **42**, 7881-7888. (d) S. A. Sydlik, Z.-H. Chen and T. M. Swager, *Macromolecules*, 2011, **44**, 976-980.

11 K. V. Rao, R. Haldar, C. Kulkarni, T. K. Maji and S. J. George, *Chem. Mater.*, 2012, **24**, 969-971.

12 M. R. Liebl and J. Senker, Chem. Mater., 2013, **25**, 970-980.

13 J. Weber, J. Schmidt, A. Thoma and W. Bohlmann, *Langmuir*, 2010, **26**, 15650-15656.

14 P. Kuhn, A. Thomas and M. Antonietti, *Macromolecules*, 2009, **42**, 319-326.

15 S.-J. Ren, R. Dawson, A. Laybourn, J.-X. Jiang, Y. Khimyak, D. J. Adams and A. I. Cooper, *Polym. Chem.*, 2012, **3**, 928-934.

16 H. A. Patel, S. H. Je, J. Park, D. P. Chen, Y. S. Jung, C. T. Yavuz and A. Coskun, *Nat. Commun.*, 2013, **4**, 1357-1364.

17 Y.-C. Zhao, Q.-Y. Cheng, D. Zhou, T. Wang and B.-H. Han, *J. Mater. Chem.*, 2012, **22**, 11509-11514.

18 (a) J.-X. Jiang, F. Su, A. Trewin, C. D. Wood, H.-J. Niu, J. T. A. Jones, Y. Z. Khimyak and A. I. Cooper, *J. Am. Chem. Soc.*, 2008, **130**, 7710-7720. (b) R. Dawson, A. I Cooper and D. J Adams, *Polym. Int.*, 2013, **62**, 345-352.

19 V. Krungleviciute, L. Heroux, A. D. Migone, C. T. Kingston and B. Simard, *J. Phys. Chem. B*, 2005, **109**, 9317-9320.

20 C. F. Martín, E Stöckel, R. Clowes, D. J. Adams, A. I. Cooper, J. J. Pis, F Rubiera and C Pevida, *J. Mater. Chem.*, 2011, **21**, 5475-5483.

21 (a) M. G. Rabbani and H. M. El-Kaderi, *Chem. Mater.*, 2011, **23**, 1650–1653. (b) M. G. Rabbani, T. E. Reich, R. M. Kassab, K, T. Jackson and H. M. El-Kaderi, *Chem. Commun.*, 2012, **48**, 1141-1143. (c) M. G. Rabbani and H. M. El-Kaderi, *Chem. Mater.*, 2012, **24**, 1511-1517.

22 (a) K. T. Jackson, M. G. Rabbani, T. E. Reich and H. M. El-Kaderi, *Polym. Chem.*, 2011, **2**, 2775-2777. (b) T. E. Reich, S. Behera, K. T. Jackson, P. Jena and H. M. El-Kaderi, *J. Mater. Chem.*, 2012, **22**, 13524-13528.

23 S. W. Yao, X. Yang, M. Yu, Y. H. Zhang and J.-X. Jiang, *J. Mater. Chem. A*, 2014, **2**, 8054-8059.

24 B.-Y. Li, Z.-H. Guan, X.-J. Yang, W. D. Wang, W. Wang, I. Hussain, K.-P. Song, B.-E. Tan and T. Li, *J. Mater. Chem. A*, 2014, **2**, 11930–11939.

25 H. Furukawa and O. M. Yaghi, *J. Am. Chem. Soc.*, 2009, **131**, 8875-8883.

26 V. C. Menon, S. Komarneni, *J. Porous. Mater.*, 1998, **5**, 43-58.

27 R. W. Tilford, S. J. Mugavero III, P. J. Pellechia and J. J. Lavigne, *Adv. Mater.*, 2008, **20**, 2741-2746.

28 M. Rose, W. Böhlmann, M. Sabo and S. Kaskel, *Chem. Commun.*, 2008, 2462-2464.

29 J. Germain, J. M. J. Fréchet and F. Svec, *J. Mater. Chem.*, 2007, **17**, 4989-4997.

30 (a) N. B. McKeown, P. M. Budd and D. Book, *Macromol. Rapid Commun.*, 2007, **28**, 995-1002. (b) B. S. Ghanem, M. Hashem, K. D. M. Harris, K. J. Msayib, M.-C. Xu, P. M. Budd, N. Chaukura, D. Book, S. Tedds, A.Walton and N. B. McKeown, *Macromolecules*, 2010, **43**, 5287-5294.

31 P. M. Budd, B. S. Ghanem, S. Makhseed, N. B. McKeown, K. J. Msayi and C. E. Tattershall, *Chem. Commun.*, 2004, 230-231.

32 Y.-L. Luo, S.-C. Zhang, Y.-X. Ma, W. Wang and B.-E. Tan, *Polym. Chem.*, 2013, **4**, 1126-1131.

Graphic abstract

This paper presents a facile and efficient method for the construction of microporous imide functionalized 1,3,5-triazine frameworks (ITFs), which exhibit high sorption capacities of CO_2, CH_4 and H_2, showing potentials in small gas separation and recovery.